



## Spectral Methods in Time for Parabolic Problems

Hillel Tal-Ezer

*SIAM Journal on Numerical Analysis*, Volume 26, Issue 1 (Feb., 1989), 1-11.

---

Your use of the JSTOR database indicates your acceptance of JSTOR's Terms and Conditions of Use. A copy of JSTOR's Terms and Conditions of Use is available at <http://www.jstor.org/about/terms.html>, by contacting JSTOR at [jstor-info@umich.edu](mailto:jstor-info@umich.edu), or by calling JSTOR at (888)388-3574, (734)998-9101 or (FAX) (734)998-9113. No part of a JSTOR transmission may be copied, downloaded, stored, further transmitted, transferred, distributed, altered, or otherwise used, in any form or by any means, except: (1) one stored electronic and one paper copy of any article solely for your personal, non-commercial use, or (2) with prior written permission of JSTOR and the publisher of the article or other text.

Each copy of any part of a JSTOR transmission must contain the same copyright notice that appears on the screen or printed page of such transmission.

*SIAM Journal on Numerical Analysis* is published by Society for Industrial and Applied Mathematics. Please contact the publisher for further permissions regarding the use of this work. Publisher contact information may be obtained at <http://www.jstor.org/journals/siam.html>.

---

*SIAM Journal on Numerical Analysis*  
©1989 Society for Industrial and Applied Mathematics

JSTOR and the JSTOR logo are trademarks of JSTOR, and are Registered in the U.S. Patent and Trademark Office. For more information on JSTOR contact [jstor-info@umich.edu](mailto:jstor-info@umich.edu).

©2000 JSTOR

## SPECTRAL METHODS IN TIME FOR PARABOLIC PROBLEMS\*

HILLEL TAL-EZER†

**Abstract.** A pseudospectral explicit scheme for solving linear, periodic, parabolic problems is described. It has infinite accuracy both in time and in space. The high accuracy is achieved while the time resolution parameter  $M$  ( $M = O(1/\Delta t)$  for time marching algorithm) and the space resolution parameter  $N$  ( $N = O(1/\Delta x)$ ) must satisfy  $M = O(N^{1+\varepsilon})$   $\varepsilon > 0$ , compared to the common stability condition  $M = O(N^2)$ , which must be satisfied in any explicit finite-order time algorithm.

**Key words.** spectral methods, explicit scheme, parabolic problems, Chebyshev expansion

**AMS(MOS) subject classification.** 65M99

**1. Introduction.** In recent years, it has been shown that spectral methods can provide a very useful tool for the solution of time-dependent partial differential equations [3]. A standard scheme uses spectral methods to approximate the space derivatives and a finite difference approach to march the solution in time. This tactic results in an unbalanced scheme; it has infinite accuracy in space and finite accuracy in time. It is obvious that the overall accuracy is influenced strongly by the relatively poor approximation of the time derivative. Moreover, using finite-order explicit scheme results in a very stringent stability condition. The timestep  $\Delta t$  must satisfy

$$(1.1) \quad \Delta t = O\left(\frac{1}{N^2}\right)$$

where  $N$  is the number of grid points in space. This severe condition is commonly overcome by resorting to implicit schemes. Varga [6] and Cody, Meinardus, and Varga [2] approached these problems by using Chebyshev rational approximations of the evolution operator. Thus, they overcome two drawbacks: low accuracy and stringent stability condition. In fact, the implicit scheme presented in [2], [6] is unconditionally stable, and the error in time decays exponentially.

Implicit algorithms involve inverting matrices. When the space approximation is based on finite differences or finite elements (as in [2], [6]), the related matrices are banded ones (e.g., tridiagonal), which makes them relatively easy to invert. On the other hand, using spectral methods for the space discretization results in full matrices. Inverting these matrices is a time-consuming procedure.

In this article we describe an explicit scheme for the solution of parabolic problems when the space discretization is done by spectral methods. This scheme is highly efficient (its efficiency is equivalent to having a stability condition  $\Delta t = O(1/N)$ ) and the error in time decays exponentially. In § 2 we present a model problem and its fully discrete solution. The new approach for approximating the evolution operator is described in § 3. In § 4 we carry out an error and stability analysis. Numerical experiments confirming the theoretical results are presented in § 5.

\* Received by the editors December 5, 1984; accepted for publication (in revised form) January 5, 1988. This research was supported in part by the National Aeronautics and Space Administration under contract NAS1-17070 while the author was in residence at the Institute for Computer Applications in Science and Engineering, NASA Langley Research Center, Hampton, Virginia 23665.

† School of Mathematical Sciences, Tel-Aviv University, Ramat Aviv, 69978 Tel Aviv, Israel. Current address, Division of Applied Mathematics, Brown University, Providence, Rhode Island 02912.

**2. The model problem.** Let us consider the heat equation

$$(2.1) \quad \begin{aligned} U_t - GU &= 0, \quad 0 < x < \Pi, \\ U(x, 0) &= U^0(x), \\ U(0, t) &= U(\Pi, t) = 0, \end{aligned}$$

where  $G$  is the spatial operator

$$(2.2) \quad G = a \frac{\partial^2}{\partial x^2}.$$

Discretizing (2.1) in space using pseudospectral Fourier method, we obtain a semi-discrete representation

$$(2.3) \quad \begin{aligned} (U_N)_t - G_N U_N &= 0, \\ U_N(x, 0) &= U_N^0(x), \\ U_N(0, t) &= U_N(\Pi, t) = 0 \end{aligned}$$

while

$$(2.4) \quad U_N = P_N U, \quad G_N = P_N G P_N, \quad U_N^0 = P_N U^0$$

and where for any function  $f(x)$ ,  $P_N f(x)$  is its sine interpolant at the collocation points

$$(2.5) \quad x_j = j\Pi/N, \quad j = 0, 1, \dots, N-1,$$

or, more precisely,

$$(2.6) \quad P_N f(x) = \sum_{k=0}^{N-1} a_k \sin(kx)$$

where

$$(2.7) \quad a_k = \frac{2}{N} \sum_{j=0}^{N-1} f(x_j) \sin(kx_j).$$

$G_N$  is an operator defined on  $N$ -dimensional subspace; thus, it can be represented as a  $N \times N$  matrix. The formal solution of (2.3) is

$$(2.8) \quad U_N(x, t) = \exp(tG_N) U_N^0(x)$$

where  $\exp(tG_N)$  is the exact evolution operator. A fully discrete solution of (2.1) is achieved by approximating this evolution operator. In [5], it has been shown that any explicit time scheme can be represented as

$$(2.9) \quad V_N^M = H_M(tG_N) U_N^0$$

where  $H_M(z)$  is a polynomial of degree  $M$  that converges to  $e^z$  in the domain that includes all the eigenvalues of the operator  $tG_N$ .  $V_N^M$  is the fully discrete solution and  $H_M(tG_N)$  is the numerical evolution operator.

**3. The orthogonal polynomials scheme.** Let  $E$  be the error that results from approximating the evolution operator. Then

$$(3.1) \quad E = [\exp(tG_N) - H_M(tG_N)] U_N^0.$$

The eigenvectors of the matrix  $tG_N$  are  $W_1, \dots, W_N$ , where  $(W_k)_j = \sin(kx_j)$ . Due to the orthogonality of this set of eigenvectors,  $tG_N$  is a normal matrix and there is an orthogonal matrix  $S_N$  such that

$$(3.2) \quad E = S_N D_N S_N^{-1} U_N^0$$

while  $D_N$  is the diagonal matrix

$$(3.3) \quad (D_N)_{kk} = e^{\lambda_k t} - H_M(\lambda_k t)$$

and  $\lambda_k t$  are the eigenvalues of  $tG_N$ . Since  $S_N$  is an orthogonal matrix, we have  $\|S_N\| = \|S_N^{-1}\| = 1$ . Therefore,

$$\|E\|_{L_2} \leq \|S_N\|_{L_2} \|D_N\|_{L_2} \|S_N^{-1}\|_{L_2} = \|D_N\|_{L_2}$$

or

$$(3.4) \quad \|E\|_{L_2} \leq \max_{z \in I} |e^z - H_M(z)|$$

where  $I$  is the domain that includes all the eigenvalues of  $tG_N$ . In our case,

$$(3.5) \quad I = [-aN^2 t, 0].$$

A standard finite-order scheme can be characterized by a polynomial  $H_M(z)$  based on a Taylor expansion of  $e^z$ . Thus, it has high accuracy only for a small  $z$ . The error increases rapidly when  $z$  is increased. This property explains the poor accuracy and stringent stability condition mentioned in the Introduction.

Let us take, for example, the modified Euler scheme. The numerical evolution operator is

$$(3.6) \quad H_M(tG_N) = (I + \Delta t G_N + \frac{1}{2}(\Delta t G_N)^2)^n$$

where

$$(3.7) \quad \Delta t = t/n.$$

Thus,

$$(3.8) \quad H_M(z) = \left( 1 + \frac{1}{n} z + \frac{1}{2n^2} z^2 \right)^n \quad (M = 2n)$$

and

$$(3.9) \quad [H_M(z)]^{1/n} = 1 + \frac{1}{n} z + \frac{1}{2n^2} z^2.$$

Equation (3.9) is the first three terms of Taylor expansion of  $e^{z/n}$ . Observing Fig. 1, we find that  $H_M(z)$  converges to  $e^z$  when

$$(3.10) \quad -2n \leq z \leq 0.$$

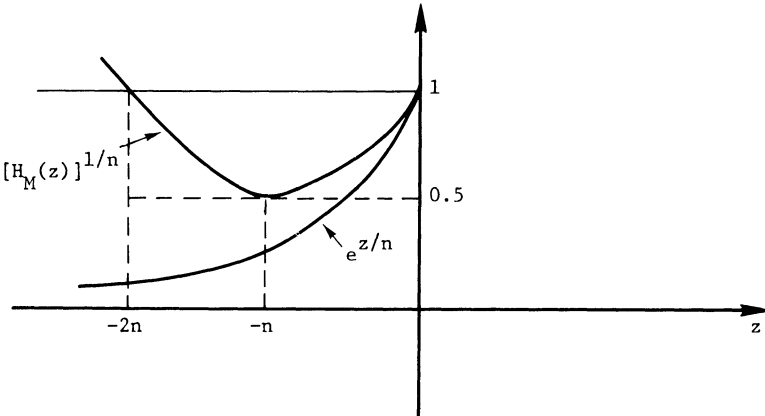


FIG. 1

(For accuracy, a more stringent condition is necessary.) Using (3.5), (3.7), and (3.10) results in the following stability condition:

$$(3.11) \quad \Delta t \leq \frac{2}{a} \left( \frac{1}{N^2} \right).$$

Expression (3.4) suggests that a uniform approximation of  $e^z$  is preferable. Such an approximation is achieved when we use Chebyshev polynomial expansion of the exponential function (see the discussion in [5] for hyperbolic problems). Let

$$(3.12) \quad w = \frac{1}{R} (z + R), \quad -1 \leq w \leq 1$$

where

$$(3.13) \quad R = \frac{1}{2} a N^2 t.$$

It then follows that

$$(3.14) \quad e^z = e^{-R} e^{Rw} = \sum_{k=0}^{\infty} b_k T_k(w)$$

where  $T_k(w)$  is the Chebyshev polynomial of order  $k$  and [1]

$$(3.15) \quad b_k = e^{-R} c_k \int_{-1}^1 e^{Rw} T_k(w) (1 - w^2)^{-1/2} dw = e^{-R} c_k I_k(R)$$

and

$$(3.16) \quad c_k = \begin{cases} 1, & k = 0, \\ 2, & k \geq 1. \end{cases}$$

$I_k(R)$  is the modified Bessel function of order  $k$ . Thus, the  $M$  degree polynomial approximation of  $e^z$  is

$$(3.17) \quad H_M(z) = \sum_{k=0}^M b_k T_k(w(z)).$$

Because of (3.12), we substitute the operator  $F_N$  defined as

$$(3.18) \quad F_N = \frac{1}{R} [t G_N + R I]$$

for  $w$ .  $H_M(F_N)$  is the numerical evolution operator. Thus, the fully discrete numerical solution of (2.1) is

$$(3.19) \quad V_N^M = H_M(F_N) U_N^0 = \sum_{k=0}^M b_k T_k(F_N) U_N^0.$$

$T_k(F_N) U_N^0$  is computed by using the recurrence relation

$$(3.20) \quad \begin{aligned} T_k(x) &= 2x T_{k-1}(x) - T_{k-2}(x), & k \geq 2, \\ T_0(x) &= 1, & T_1(x) = x. \end{aligned}$$

Hence,

$$(3.21) \quad \begin{aligned} T_k(F_N) U_N^0 &= 2 F_N T_{k-1}(F_N) U_N^0 - T_{k-2}(F_N) U_N^0, & k \geq 2, \\ T_0(F_N) U_N^0 &= U_N^0, & T_1(F_N) U_N^0 = F_N U_N^0. \end{aligned}$$

The algorithm defined by (3.19), (3.21) can be regarded as a three-level scheme since it uses the recurrence relation. Therefore, it has the disadvantage of requiring extra memory. There are two possible ways to overcome this drawback. The first is to convert (3.19) to a power series in  $F_N$  and use the Horner scheme to compute  $V_N^M$ . The disadvantage of this approach is its sensitivity to roundoff errors. The second is based on calculating the roots of  $H_M(w)$ . Let us assume that the roots are

$$(3.22) \quad \theta_1, \dots, \theta_M.$$

Since the  $b_k$  are real, every complex root appears with its conjugate. Rearranging (3.22) in such a way that the first  $2p$  roots are  $p$  conjugate pairs, we get

$$(3.23) \quad \mu_1, \bar{\mu}_1, \dots, \mu_p, \bar{\mu}_p, \mu_{p+1}, \dots, \mu_{M-p}.$$

Thus

$$(3.24) \quad H_M(w) = \alpha_0 \prod_{i=1}^p (1 - \alpha_i w + \beta_i w^2) \prod_{i=p+1}^{M-p} (1 - \gamma_i w),$$

while

$$(3.25) \quad \begin{aligned} \alpha_0 &= \sum_{k=0}^{M/2} b_k, \\ \beta_i &= 2R_e \mu_i / |\mu_i|^2, \quad \beta_i = 1/|\mu_i|^2, \quad 1 \leq i \leq p, \\ \gamma_i &= 1/\mu_i, \quad p+1 \leq i \leq M-p. \end{aligned}$$

Hence we get

$$(3.26) \quad H_M(F_N) = \alpha_0 \prod_{i=1}^p [I - \alpha_i F_N + \beta_i F_N^2] \prod_{i=p+1}^{M-p} [I - \gamma_i F_N] U_N^0.$$

Each algorithm described above can be used as a one-step method by calculating the solution at the final time  $t$  directly from the initial data. It can also be used as a marching scheme when considering intermediate results. The size of the timestep  $\Delta t$  depends only on the information we want to obtain from the numerical procedure.  $\Delta t$  enters instead of  $t$  in the expressions above, and the parameter  $R$  is determined accordingly. In any case, the refinement of the algorithm is done by increasing the degree of the polynomial and not by decreasing the size of the timestep.

**4. Accuracy and stability.** Using (3.4), (3.15), and (3.17), we get

$$(4.1) \quad \|E\|_{L_2} \leq 2 e^{-R} \left| \sum_{k=M+1}^{\infty} I_k(R) T_k(w) \right|, \quad -1 \leq w \leq 1.$$

Since  $e^{Rw}$  is an entire function, it satisfies the following theorem ([4, pp. 94–96]).

**THEOREM** (S.N. Bernstein). *Let  $f(w)$  be an entire transcendental function that is real for real  $w$ . Then there exists a sequence of integers  $n_1, n_2, \dots$  with  $n_\mu \rightarrow \infty$  such that the relation*

$$(4.2) \quad \lim_{\mu \rightarrow \infty} \frac{E_{n_\mu}(f)}{|\alpha_{n_\mu} + 1|} =$$

holds, where  $\alpha_k$  are the coefficients in the expansion

$$(4.3) \quad f(w) = \frac{\alpha_0}{2} + \sum_{k=1}^{\infty} \alpha_k T_k(w)$$

and

$$(4.4) \quad E_n(f) = \left| f(w) - \frac{\alpha_0}{2} - \sum_{k=1}^n \alpha_k T_k(w) \right|.$$

There is a sequence of integers  $n_\mu$ ,  $\mu = 1, 2, \dots$  of the above type provided

$$(4.5) \quad (1) \quad \alpha_{n_\mu+1} \neq 0, \quad \mu = 1, 2, \dots, \text{ and}$$

$$(4.6) \quad (2) \quad \sum_{k=n_\mu+2}^{\infty} |\alpha_k| = O(|\alpha_{n_\mu+1}|) \quad \text{as } \mu \rightarrow \infty.$$

In our case we can take  $n_\mu = \mu$ ,  $\mu = 1, 2, \dots$ , and it follows that

$$(4.7) \quad \|E\|_{L_2} \leq 2 e^{-R} I_{M+1}(R) (1 + O(1)).$$

The asymptotic expansion of  $I_k(R)$  is [1]:

$$(4.8) \quad I_k(R) \sim \frac{e^R}{\sqrt{2\pi R}} \left\{ 1 - \frac{\mu-1}{8R} + \frac{(\mu-1)(\mu-9)}{2!(8R)^2} - \frac{(\mu-1)(\mu-9)(\mu-25)}{3!(8R)^3} + \dots \right\}$$

where

$$(4.9) \quad \mu = 4k^2.$$

Hence,

$$(4.10) \quad 2 e^{-R} I_k(R) \sim \sqrt{\frac{2}{\pi R}} \left[ 1 - \frac{\mu}{8R} + \frac{1}{2!} \left( \frac{\mu}{8R} \right)^2 - \dots + O\left(\frac{1}{R}\right) \right]$$

or

$$(4.11) \quad 2 e^{-R} I_k(R) \sim \sqrt{\frac{2}{\pi R}} \exp(-\mu/8R) + O(R^{-3/2}).$$

From (4.7), (4.9), and (4.11), we conclude that an  $\varepsilon$  time accuracy,

$$(4.12) \quad \|E\|_{L_2} \leq \varepsilon,$$

is achieved when

$$(4.13) \quad M = O(R^{1/2}).$$

It is clear that satisfying (4.13) guarantees stability. In fact, using (3.1), (4.12), we get

$$(4.14) \quad \|\exp(tG_N) - H_M(tG_N)\| \leq \varepsilon;$$

hence,

$$(4.15) \quad \|H_M(tG_N)\| \leq \|\exp(tG_N)\| + \varepsilon.$$

Since  $\exp(tG_N)$  is a stable operator [3],  $H_M(tG_N)$  is stable as well.

$R$  is equal to  $aN^2 t/2$ ; thus from (4.13) we can conclude the main result of this analysis. In order to achieve  $\varepsilon$  time accuracy, stable solution of (2.3),  $M$  must satisfy

$$(4.16) \quad M = O(N).$$

A similar analysis for any finite-order scheme based on Taylor expansion of  $e^z$  will imply that  $M$  [ $M = O(1/\Delta t)$ ; see (3.7)–(3.8)] must be proportional to  $N^2$ , thus the advantage of the orthogonal polynomials approach is obvious.

**ALGORITHM REFINEMENT.** From (3.13), (4.7), (4.9), and (4.11), we get

$$(4.17) \quad E \approx \frac{2}{N} \left( \frac{1}{a\pi t} \right)^{1/2} \exp \left( -\frac{(M/N)^2}{at} \right).$$

Expression (4.17) suggests refinement of the algorithm while

$$(4.18) \quad M = N^\alpha \quad (\alpha > 1)$$

will yield an exponential decay of the error. The accuracy thus achieved is the desired spectral accuracy.

**5. Numerical results.** Table 1 presents the stability properties of the OPS (Orthogonal Polynomial Scheme) compared to the modified Euler scheme, which is second order in time. We used the model problem (2.1) with  $a = 1$ , and initial data

$$(5.1) \quad U^0(x) = \sin(3x).$$

The solution is computed at  $t = 1$ .  $M$  indicates the minimal number of applications of the operator  $tG_N$  we must use to achieve stable (meaningful) results.

Table 2 clarifies the spectral convergence of the OPS scheme. In this table we included the results for the modified Euler scheme as well for the sake of comparison. The problem solved is

$$(5.2) \quad \begin{aligned} U_t - U_{xx} &= 0, & 0 \leq x \leq 2\pi, \\ U^0(x) &= x(x - 2\pi), \end{aligned}$$

Note that the periodic continuation of  $U^0(x)$  belongs to  $C^0$ ; thus the Fourier coefficients of  $U^0(x)$  are decaying slowly. The solution is computed at  $t = 1$ . The refinement of the modified Euler scheme is done while  $M$  satisfies

$$M = 0.97 \times (N/2)^2.$$

For the OPS algorithm,  $M$  satisfies

$$M = 2.5 \times (N/2)^{1.2}.$$

TABLE 1

$N$	Modified Euler $M$	OPS $M$
16	48	24
32	192	48
64	768	96

TABLE 2

$N$	Modified Euler			OPS		
	$M$	$L_2$ -error	Ratio	$M$	$L_2$ -error	Ratio
16	62	.3791 - 04	17.4	26	.1026 - 04	92
32	250	.2126 - 05	16.2	61	.1107 - 06	134
64	1000	.1339 - 06		140	.8263 - 09	

The increasing ratio between the  $L_2$ -errors of two successive refinements verifies the spectral convergence of the OPS algorithm.

In Table 3 we compare the OPS to the modified Euler scheme from the point of view of the amount of work needed to achieve a certain degree of accuracy. The problem solved is  $U_t - U_{xx} = 0$  with  $U^0(x) = \sin(3x)$ . The  $L_2$ -error is computed at the time level  $t = 1$ , and the space resolution is  $N = 32$ .

In the next set of numerical experiments we used our algorithm to solve a variable coefficient problem, which can be presented as follows:

$$(5.3) \quad \begin{aligned} (u_N)_t - G_N u_N &= s_1(x) + ts_2(x), \\ u_N(x, 0) &= u_N^0(x), \end{aligned}$$

while

$$(5.4a) \quad G_N = P_N G P_N,$$

$$(5.4b) \quad G = a(x) \frac{\partial^2}{\partial x^2} + b(x) \frac{\partial}{\partial x} + c(x).$$

If the exact solution of (5.3) is

$$(5.5) \quad u_N(x, t) = ts(x),$$

then

$$(5.6) \quad u_N^0(x) = 0,$$

$$(5.7) \quad s_1(x) = s(x),$$

$$(5.8) \quad s_2(x) = -G_N(S_1(x)).$$

The formal solution of (5.3) is

$$(5.9) \quad u = f_0(G_N t)u_N^0 + f_1(G_N t)s_1 + f_2(G_N t)s_2$$

where

$$(5.10) \quad f_0(G_N t) = \exp(G_N t),$$

$$(5.11) \quad f_1(G_N t) = \int_0^t \exp(G_N \tau) d\tau = t(G_N t)^{-1}(\exp(G_N t) - I),$$

$$(5.12) \quad f_2(G_N t) = \int_0^t \exp(G_N \tau)(t - \tau) d\tau = t^2(G_N t)^{-2}(\exp(G_N t) - G_N t - I).$$

Since  $u_N^0 = 0$ , the first term on the right-hand side of (5.9) is zero. Thus, in order to implement our algorithm we have to approximate the following functions:

$$(5.13) \quad f_1(zt) = \int_0^t e^{z\tau} d\tau = t \frac{e^{zt} - 1}{zt} = t \tilde{f}_1(zt), \quad z \in D,$$

$$(5.14) \quad f_2(zt) = \int_0^t e^{z\tau}(t - \tau) d\tau = t^2 \frac{e^{zt} - zt - 1}{(zt)^2} = t^2 \tilde{f}_2(zt), \quad z \in D$$

TABLE 3

$L_2$ -error	$M$ (modified Euler)	$M$ (OPS)
$1.3 \times 10^{-2}$	200	50
$1.3 \times 10^{-4}$	2,000	60
$1.3 \times 10^{-6}$	20,000	70

where  $D$  is the domain in the complex plane that contains the eigenvalues of the operator  $G_N$ . The domain  $D$  can be approximated by doing a Fourier analysis of the constant coefficients operator

$$(5.15) \quad \tilde{G} = a \frac{\partial^2}{\partial x^2} + b \frac{\partial}{\partial x} + c$$

where

$$(5.16a) \quad a = \max |a(x)|,$$

$$(5.16b) \quad b = \max |b(x)|,$$

$$(5.16c) \quad c_{\max} = \max |c(x)|; \quad c_{\min} = \min |c(x)|.$$

We get

$$(5.17) \quad \tilde{D} = \{x + iy \mid -(N^2 + c_{\max}) \leq x \leq -c_{\min}, |y| \leq b\}.$$

Since

$$(5.18) \quad N^2 + C_{\max} \gg b,$$

using the domain  $\tilde{D}$  where

$$(5.19) \quad \tilde{D} = \{x \mid -(N^2 + c_{\max}) \leq x \leq -c_{\min}\},$$

we obtain a good approximation of  $D$ . In order to write  $\tilde{f}_1, \tilde{f}_2$  as a Chebyshev polynomial expansion we first must change variables. Define

$$(5.20) \quad z = R w + Q, \quad -1 \leq w \leq 1$$

where

$$(5.21) \quad R = \frac{1}{2}[N^2 + c_{\max} - c_{\min}],$$

$$(5.22) \quad Q = -\frac{1}{2}[N^2 + c_{\max} + c_{\min}];$$

then

$$(5.23) \quad \tilde{f}_1(zt) = \hat{f}_1(wt) = \frac{e^{Qt} e^{Rtw} - 1}{Rtw + Qt} = \sum_{k=0}^{\infty} d_k T_k(w),$$

$$(5.24) \quad \tilde{f}_2(zt) = \frac{1}{zt} [\tilde{f}_1(zt) - 1] = \frac{\hat{f}_1(wt) - 1}{Rtw + Qt} = \sum_{k=0}^{\infty} g_k T_k(w).$$

From (3.14), (3.15), (3.16) we have

$$(5.25) \quad e^{Rtw} = \sum_{k=0}^{\infty} b_k T_k(w),$$

while

$$(5.26) \quad b_k = c_k I_k(Rt), \quad c_k = \begin{cases} 1, & k=1, \\ 2, & k \geq 2, \end{cases}$$

and  $I_k$  are modified Bessel functions. Substituting (5.25) in (5.13) and (5.24), we get

$$(5.27) \quad R w \sum_{k=0}^{\infty} d_k T_k + Q \sum_{k=0}^{\infty} d_k T_k = \frac{1}{t} \left[ \sum_{k=0}^{\infty} \tilde{b}_k T_k - 1 \right] \quad (\tilde{b}_k = e^{Qt} b_k),$$

$$(5.28) \quad R w \sum_{k=0}^{\infty} g_k T_k + Q \sum_{k=0}^{\infty} g_k T_k = \frac{1}{t} \left[ \sum_{k=0}^{\infty} d_k T_k - 1 \right].$$

Since Chebyshev polynomials satisfy the recurrence relation

$$(5.29) \quad T_{k+1} = 2wT_k - T_{k-1},$$

we get

$$(5.30) \quad wT_k = \frac{1}{2}(T_{k+1} + T_{k-1}).$$

Using (5.30) in (5.27), (5.28) results in tridiagonal systems of equations for the two sets of unknowns:

$$\{d_k\}, \quad \{g_k\}, \quad 0 \leq k \leq N/2.$$

In our numerical experiments, we used

$$(5.31) \quad s_1(x) = \exp(-4(x - \pi)^2),$$

$$(5.32) \quad a(x) = 1. / (2. + \cos x),$$

$$(5.33) \quad b(x) = 1. / (2. + \sin x),$$

$$(5.34) \quad c(x) = -20. / (2. + \cos x).$$

The results at  $t = 1$  are presented in Table 4.

We also used the OPS algorithm to compute the solution at  $t = 10$ , and the results are presented in Table 5.

Observing Tables 4 and 5, we notice that  $M$  does not depend on  $t$ . This can be explained as follows. For large  $t$ ,  $\|\exp(G_N t)\|$  is very small. Thus, since (5.11), (5.12), we have

$$(5.35) \quad \tilde{f}_1(G_N t) \approx -G_N^{-1},$$

$$(5.36) \quad \tilde{f}_1(G_N t) \approx -G_N^{-2}(G_N t + I),$$

which means that for large  $t$ , approximating  $\tilde{f}_1(G_N t)$  is equivalent to inverting  $G_N$  and approximating  $\tilde{f}_2(G_N t)$  is equivalent to inverting  $(G_N)^2$ .

**6. Conclusion.** The algorithm presented in this paper achieves the goal of spectral accuracy in time and space for the simple model problem (2.1). We believe that this approach can be useful for more complicated problems. In fact, the scheme described in § 3 is applicable whenever we can represent the solution as  $\exp(tG_N)U_N$  and the eigenvalues of  $tG_N$  are grouped close to the real axis.

TABLE 4

Modified Euler			OPS	
$N$	$M$	$L_2$ -error	$M$	$L_2$ -error
16	30	.4885 - 01	16	.4885 - 01
32	120	.1250 - 05	40	.1173 - 05
64	480	.1296 - 05	100	.1258 - 08

TABLE 5

$N$	$M$	$L_2$ -error (OPS)
16	16	.5358 - 01
32	40	.2377 - 05
64	110	.3968 - 07

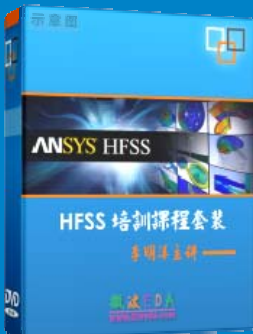
## REFERENCES

- [1] M. ABRAMOWITZ AND I. A. STEGUN, *Handbook of Mathematical Functions*, Dover, New York, 1972.
- [2] W. J. CODY, G. MEINARDUS, AND R. S. VARGA, *Chebyshev, rational approximations to heat—conduction problems*, J. Approx. Theory, 2 (1969), pp. 50–65.
- [3] D. GOTTLIEB AND S. ORSZAG, *Numerical Analysis of Spectral Methods: Theory and Applications*, CBMS-NSF Regional Conference Series in Applied Mathematics 26, Society for Industrial and Applied Mathematics, Philadelphia, PA, 1972.
- [4] G. MEIMARDUS, *Approximation of Functions: Theory and Numerical Methods*. Springer-Verlag, Berlin, New York, 1967.
- [5] H. TAL-EZER, *Spectral methods in time for hyperbolic problems*, SIAM J. Numer. Anal., 23 (1986), pp. 11–26.
- [6] R. S. VARGA, *Functional Analysis and Approximation Theory in Numerical Analysis*, CBMS-NSF Regional Conference Series in Applied Mathematics 3, Society for Industrial and Applied Mathematics, Philadelphia, PA, 1971.

## HFSS 视频培训课程推荐

HFSS 软件是当前最流行的微波无源器件和天线设计软件，易迪拓培训([www.edatop.com](http://www.edatop.com))是国内最专业的微波、射频和天线设计培训机构。

为帮助工程师能够更好、更快地学习掌握 HFSS 的设计应用，易迪拓培训特邀李明洋老师主讲了多套 HFSS 视频培训课程。李明洋老师具有丰富的工程设计经验，曾编著出版了《HFSS 电磁仿真设计应用详解》、《HFSS 天线设计》等多本 HFSS 专业图书。视频课程，专家讲解，直观易学，是您学习 HFSS 的最佳选择。



### HFSS 学习培训课程套装

该套课程套装包含了本站全部 HFSS 培训课程，是迄今国内最全面、最专业的 HFSS 培训教程套装，可以帮助您从零开始，全面深入学习 HFSS 的各项功能和在多个方面的工程应用。购买套装，更可超值赠送 3 个月免费学习答疑，随时解答您学习过程中遇到的棘手问题，让您的 HFSS 学习更加轻松顺畅…

课程网址: <http://www.edatop.com/peixun/hfss/11.html>

### HFSS 天线设计培训课程套装

套装包含 6 门视频课程和 1 本图书，课程从基础讲起，内容由浅入深，理论介绍和实际操作讲解相结合，全面系统的讲解了 HFSS 天线设计的全过程。是国内最全面、最专业的 HFSS 天线设计课程，可以帮助您快速学习掌握如何使用 HFSS 设计天线，让天线设计不再难…

课程网址: <http://www.edatop.com/peixun/hfss/122.html>



### 更多 HFSS 视频培训课程:

#### ● 两周学会 HFSS —— 中文视频培训课程

课程从零讲起，通过两周的课程学习，可以帮助您快速入门、自学掌握 HFSS，是 HFSS 初学者的最好课程，网址: <http://www.edatop.com/peixun/hfss/1.html>

#### ● HFSS 微波器件仿真设计实例 —— 中文视频教程

HFSS 进阶培训课程，通过十个 HFSS 仿真设计实例，带您更深入学习 HFSS 的实际应用，掌握 HFSS 高级设置和应用技巧，网址: <http://www.edatop.com/peixun/hfss/3.html>

#### ● HFSS 天线设计入门 —— 中文视频教程

HFSS 是天线设计的王者，该教程全面解析了天线的基础知识、HFSS 天线设计流程和详细操作设置，让 HFSS 天线设计不再难，网址: <http://www.edatop.com/peixun/hfss/4.html>

#### ● 更多 HFSS 培训课程，敬请浏览: <http://www.edatop.com/peixun/hfss>

## 关于易迪拓培训:

易迪拓培训([www.edatop.com](http://www.edatop.com))由数名来自于研发第一线的资深工程师发起成立，一直致力于专注于微波、射频、天线设计研发人才的培养；后于 2006 年整合合并微波 EDA 网([www.mweda.com](http://www.mweda.com))，现已发展成为国内最大的微波射频和天线设计人才培养基地，成功推出多套微波射频以及天线设计相关培训课程和 ADS、HFSS 等专业软件使用培训课程，广受客户好评；并先后与人民邮电出版社、电子工业出版社合作出版了多本专业图书，帮助数万名工程师提升了专业技术能力。客户遍布中兴通讯、研通高频、埃威航电、国人通信等多家国内知名公司，以及台湾工业技术研究院、永业科技、全一电子等多家台湾地区企业。

## 我们的课程优势:

- ※ 成立于 2004 年，10 多年丰富的行业经验
- ※ 一直专注于微波射频和天线设计工程师的培养，更了解该行业对人才的要求
- ※ 视频课程、既能达到现场培训的效果，又能免除您舟车劳顿的辛苦，学习工作两不误
- ※ 经验丰富的一线资深工程师讲授，结合实际工程案例，直观、实用、易学

## 联系我们:

- ※ 易迪拓培训官网: <http://www.edatop.com>
- ※ 微波 EDA 网: <http://www.mweda.com>
- ※ 官方淘宝店: <http://shop36920890.taobao.com>